Microbial Cell Factories

RESEARCH

Open Access

The potential application of isoxanthohumol in inhibiting *Clostridium perfringens* infection by targeting the type IV pili

Zeyu Song[1†], Yanhong Deng[1†], Jichuan Zhang[1], Zhongmei Wen[2], Shui Liu[3], Xuming Deng[1], Qiaoling Zhang[1*] and Qianghua Lv[1,4,5*]

Abstract

Background *Clostridium perfringens* (*C. perfringens*) is an important zoonotic pathogen. The diseases such as necrotic enteritis (NE), enterotoxemia, gas gangrene and food poisoning caused by its infection seriously threaten the lives of both humans and animals. However, under the severe situation of antibiotic resistance, the development of new antibacterial strategies or drugs deserves great attention.

Results In this study, we selected the virulence factor Type IV pili (TFP) of *C. perfringens* as the target for drug screening. The gliding motility, biofilm formation, cell adhesion and antibacterial activity of the natural compound isoxanthohumol (IXN) against *C. perfringens* were determined. Transmission electron microscopy (TEM), TFP gene transcription analysis and Western blot were used to detect the expression of PilA pilin. The therapeutic effect of IXN on *C. perfringens* infection was demonstrated through a mouse gas gangrene model. It was confirmed that IXN inhibits the function of TFP by down-regulating TFP-encoding genes and two-component regulatory genes.

Conclusions In conclusion, our study shows that IXN has the potential to inhibit the function of TFP in *C. perfringens* and for anti-infection applications.

Keywords *C. perfringens*, Zoonotic pathogen, Isoxanthohumol, TFP, Anti-infection

Introduction

C. perfringens is a Gram-positive, anaerobic and aerotolerant rod-shaped bacterium, which is one of the most common pathogens in nature. It can be isolated from the gastrointestinal tracts of human and animals, and widely distributed in soil, sewage and rotten organic matter. The diseases caused by *C. perfringens* in humans mainly include gas gangrene, food poisoning, necrotizing enterocolitis (NE), etc. Its harm to the livestock and poultry breeding industry, as well as gas gangrene and enterotoxemia in mammals such as sheep, goats, cattle and horses [1–3]. The pathogenicity of *C. perfringens* is related to the multiple extracellular toxins (13 different toxins have been reported so far) [4]. It causes diseases by secreting extracellular toxins to damage the small intestinal mucosa of the host, and includes gas gangrene when

†Zeyu Song and Yanhong Deng contributed equally to this work.

*Correspondence:
Qiaoling Zhang
zql@jlu.edu.cn
Qianghua Lv
lvqianghua129@jlu.edu.cn
[1] Key Laboratory of Zoonosis Research, Ministry of Education, Institute of Zoonosis, College of Veterinary Medicine, Jilin University, Changchun 130062, China
[2] Department of Respiratory Medicine, The First Hospital of Jilin University, Jilin University, Changchun 130062, China
[3] Department of Pathogenic Biology, Jilin Medical University, Jilin, China
[4] Shandong Key Laboratory of Animal Disease Control and Breeding, Institute of Animal Science and Veterinary Medicine, Shandong Academy of Agricultural Sciences, Jinan, People's Republic of China
[5] Key Laboratory of Livestock and Poultry Multi-Omics of MARA, Jinan, People's Republic of China

invading muscle tissues or loose connective tissues [5]. Its characteristics are mainly manifested as tissue necrosis and gas production, and shock and organ failure are also common late-stage complications, with a predicted mortality rate of over 50% [6]. In humans, gas gangrene is divided into spontaneous gangrene and traumatic gangrene. The former is usually caused by *C. perfringens*, while the latter is mostly caused by open injuries, with a mortality rate of about 80% [7].

Type IV pili (TFP) is one of the most important virulence factors in the infection process of *C. perfringens* [8]. It has been reported that TFP mediates multiple biological functions, such as gliding motility, adhesion to host cells, DNA uptake and protein secretion [9]. The genome of *C. perfringens* contains multiple gene clusters that jointly encode TFP, such as *pilA*, *pilD*, *pilB*, *pilC* and *pilT*. The main structure of TFP is composed of PilA pilin, which are translated from several pilin genes (*pilA1*, *pilA2-1*, *pilA2-2*) [10]. PilD is a peptidase that recognizes PilA and modifies pili precursor protein. PilB is an ATPase responsible for providing energy for pilus assembly [11, 12]. *PilC* (described as the gene encoding the inner membrane core protein) is usually paired with *pilB* [11, 12]. It is speculated that there may be some unknown interactions between PilC and pilB [10]. PilT is also an ATPase that provides energy for pilus contraction. Adhesion and colonization are the main prerequisites for *C. perfringens* infection [10]. The process of adhesion promotes pathogenic bacteria to resist the flushing of intestinal mucus, the movement of cilia and the peristalsis of the intestine, ensuring colony colonization. TFP modulates adhesion and cell damage of *C. perfringens*, and provides assurance for the gliding motility of *C. perfringens* on solid or culture medium surfaces. In addition, TFP is one of the main prerequisites for biofilms formation, and the ability to biofilms formation in mutant strains with gene deletion of pili T and pili C is significantly reduced [13, 14]. It has been confirmed that the mutants lacking TFP or gliding motility have serious defects in adhesion, resulting in significantly reduced for pathological damage. Therefore, TFP can be used as a potential target for the prevention and treatment of *C. perfringens* infection, and targeting TFP and inhibiting the biological functions may be an ideal choice for treating infections.

Traditional antibiotic research involves disrupting the vitality through antibacterial or bactericidal molecules. It should be noted that the virulence factors of *C. perfringens*, such as TFP and related coding and regulatory systems, are usually not essential components for bacterial survival [9]. The key to developing strategies to replace or supplement antibiotics targeting bacterial virulence factors is to seek potential drugs that can disrupt or reduce bacterial virulence. More importantly, drugs targeting virulence factors exert extremely small selective pressure on the emergence and evolution of bacterial resistance and have little impact on the genetic evolution and spread of resistance.

We screened traditional plant natural compounds and successfully obtained a potential inhibitor of TFP. We also characterized its pharmacological effects both in vitro and in vivo. We identified an isoprenylated flavonoid, isoxanthohumol (IXN), which is a natural compound in the *Humulus lupulus Linn* plants growing in the northwest and southwest regions of China. It has a wide range of biological characteristics, such as anti-inflammatory, antioxidant stress, regulation lipid metabolism, and ant-infection [15–18]. In this study, we investigated the effects of IXN on gliding motility, biofilm formation and adherence to Caco-2 cells of *C. perfringens*. The results showed that IXN down-regulated the expression of TFP-encoding genes and two-component regulation system genes, and it had a good therapeutic effect on gas gangrene caused by *C. perfringens* in mouse. This study demonstrated that TFP is an ideal target for combating the pathogenicity of *C. perfringens* and drug development, and it also indicated that IXN has good potential for anti-infection.

Materials and methods

Strains, compounds and cultivating conditions

Isoxanthohumol (purity > 98%, IXN) was purchased from Herbpurify CO. LTD (Chengdu, China) and dissolved in dimethyl sulfoxide (DMSO, Sigma-Aldrich, St. Louis, USA) to prepare the standard solution. *C. perfringens* strain ATCC13124 (a gas gangrene strain isolated from human) was derived from the American Type Culture Collection (ATCC) and stored in our laboratory. The bacteria were cultured in BHI (Hope Biol-Technology, Qingdao, China) broth at 37℃.

Gliding motility assay

0.7% agar BHI solid plate containing different final concentrations of IXN was prepared. Meanwhile, the control groups were set up respectively with DMSO only and without IXN. *C. perfringens* ATCC13124 was cultured in an anaerobic environment at 37 °C in a 2.5 L vertical anaerobic culture bag (Hope Biol-Technology, Qingdao, China). 1 mL of the culture was incubated overnight (ON) and then centrifugated at 12,000 rpm for 10 min. After that, the supernatant was discarded, and the pellet was re-suspended in 100 μL of BHI medium to prepare the bacterial suspension. 10 μL of the bacterial suspension was added to the center of the plate and incubated for 96 h at 37 °C. Subsequently, the diameter of the bacteria gliding motility was measured.

Antibacterial activity assays

The ON culture of *C. perfringens* ATCC13124 was adjusted to an optical density (OD) of 600 nm equal to 0.1 using BHI medium. Subsequently, IXN was introduced into the culture to achieve final concentrations of 0, 4, 8, 16, 32, and 64 μg/mL respectively. The bacteria were then cultivated in an anaerobic environment at 37 °C, and theOD600nm was measured at 1-h intervals until the culture reached the stationary phase. The minimum inhibitory concentrations (MICs) of IXN against *C. perfringens* ATCC13124 were determined by referring to the agar dilution method as described by the Clinical and Laboratory Standards Institute (CLSI 2012) [19].

Biofilm formation assays

The ON culture of *C. perfringens* ATCC13124 was centrifuged at 12,000 rpm for 10 min. Subsequently, the supernatant was carefully removed, and the cell pellet was washed thrice with phosphate-buffered saline (PBS, pH = 7.4). Following the washing procedure, the cells were re-suspended in tryptic soy broth (TSB) to attain an OD600nm of precisely 0.1. The re-suspended culture was then aliquoted into 24-well plates, with each well containing 400 μL of the culture. IXN was added to the wells to achieve a range of concentrations from 0 to 16 μg/mL. The plates were then placed in an anaerobic environment and cultured at 30 °C for 120 h to facilitate biofilm formation. Then the OD600nm of the culture supernatant in each well of the 24-well plate was measured. Subsequently, the wells were gently washed with PBS for three times and then allowed to dry at room temperature for 1 h. To visualize and quantify the formed biofilms, 400 μL of a 0.1% crystal violet solution was added to each well, and the biofilms were stained for a duration of 1 h. Following the staining process, the residual crystal violet was removed by washing three times with PBS. Subsequently, an equal volume of a 33% glacial acetic acid solution was added to each well to dissolve the crystal violet. Then, 100 μL of the dissolved crystal violet solution was transferred from each well to a 96-well plate. Finally, the quantification of the biofilms was accomplished by measuring the absorbance at 570 nm using a microplate reader (Tecan, Grödig, Austria).

Evaluation of the resistance of biofilm and planktonic bacteria to oxidative stress

C. perfringens was prepared following the procedures described previously. After a period of 5 days, the biofilm and planktonic populations were quantified from a designated set of tissue culture plates. For the biofilm, it was washed with PBS containing 0.25% trypsin to effect dissolution. Subsequently, both the supernatant and the biofilm dissolution solution were diluted using PBS and then spread onto BHI plates for colony counting, thereby determining the initial bacterial count. The second group of samples was cultured in an anaerobic environment for 4 days and subsequently transferred to an aerobic environment for a period of 24 h. Subsequently, colonies were counted following the same method as described above. The remaining two groups of samples were first exposed to an aerobic environment for 24 h. Subsequently, they were treated with 5 mM hydrogen peroxide (H_2O_2) for a duration of 5 min. After treatment, colonies were counted on BHI plates following the same procedure as detailed above.

Cell culture and cytotoxicity assay

The human intestinal epithelial cell line Caco-2 was cultured in Dulbecco's modified Eagle's medium (DMEM, Sigma Aldrich, St. Louis, USA), which was supplemented with 10% fetal bovine serum (FBS, Biological Industries, Kibbutz Beit-Haemek, Israel) and penicillin–streptomycin (except for infection assays) at 37 °C in a 5% CO_2 humidified atmosphere.

We assessed the cytotoxicity of IXN by determining the release of lactate dehydrogenase (LDH) in the supernatant [20]. Briefly, Caco-2 cells were seeded in 96-well plates at a density of 2×10^4 in 200 μL. Subsequently, the cells were incubated with different concentrations of IXN (0, 4, 8, 16 and 32 μg/mL) for 24 h at 37 °C. The cytotoxicity then quantified using the Cytotoxicity Detection kit (Roche Diagnostics, Mannheim, Germany) with a microplate reader (Tecan, Grödig, Austria) at a wavelength of 490 nm.

Adherence assays

Caco-2 cells were seeded in 24-well plates at a density of 1×10^5 and cultured overnight at 37 °C in an atmosphere containing 5% CO_2. Subsequently, the cells were gently washed with PBS. Next, 1 mL of the ON culture of *C. perfringens* was prepared and its OD600nm was adjusted to 0.3. IXN or DMSO was then added to these cultures to achieve final concentrations ranging from 0 to 32 μg/mL. The cultures were then incubated anaerobically for 2 h at 37 °C. After incubation, the cells were washed three times with PBS to remove the non-adhered bacteria. Subsequently, the cells were lysed using 0.2% (volume/volume) Triton X-100. The resulting bacterial solution was then diluted on BHI plates and enumerated after overnight anaerobic culture at 37 °C.

Transmission electron microscopy (TEM) and TFP-associated genes expression analysis

As previously described, the impact of IXN on the pili morphology of *C. perfringens* ATCC13124 was

examined through TEM [21]. Briefly, formvar carbon-coated copper grids were utilized to coat the bacterial precipitates. Subsequently, a drop of 2% sodium phosphotungstate solution was added for fixation, which lasted for 15 min. After being left at room temperature for approximately 3–5 min, the excess water was carefully absorbed. Once dried, the samples were placed under a TEM (Hitachi HT7800, Japan) to observe the pili morphology.

RT-PCR was carried out to analyze the expression levels of genes associated with TFP (*pilA*, *pilA2, pilM*, *pilC*, *pilD* and *pilT*), two-comment regulation system genes (*virR*/*virS*) and downstream gene (*pfoA, plc, colA and netB*). The ON culture of *C. perfringens* ATCC13124 was adjusted to an OD600 nm equal to 0.3. The bacterial culture was then co-cultured with different concentrations (0 μg/mL and 16 μg/mL) of IXN until it reached the stationary phase, and a DMSO control group was established. The bacteria were collected by centrifugation at 12,000 rpm for 2 min. Next, the total RNA of *C. perfringens* was extracted using trizol reagent. Subsequently, cDNA was synthesized using the One-Step gDNA Removal and cDNA Synthesis Super Mix (Transgene, China). The expression of TFP-associated genes was quantified by Applied Biosystems Real-Time PCR Systems (Applied biosystems, Carlsbad, USA). The housekeeping gene *16S rRNA* was employed as an internal control, and the primers used were shown in Table 1.

Table 1 Primers used in this study

Target	Primer sequence (5′-3′)	Product size (bp)
virR	F: ACACAAGCTGTAACCTGCTCT R: TGGGTGAGTTAACAGGAATGGA	128
virS	F: TCCAAAACCTTCTCGTCCCC R: TCGTGTAGATATTGGAAAGGGAGA	92
pilA1	F: ACTTTTGCCTTAGCGCTATCC R: TGTGGAAAAGGAAATGAAGGGA	102
pilC1	F: AGCCTTTGATAAAGCTTCTCCAT R: GGAATGCCTATAGGACGATCATT	82
pilD	F: TCTCCACTCCCCATAGCTCC R: ACCCAGCTGTAATACTTGGGA	93
pilM	F: TCCAAAGCGTCATTAATAGCCA R: ACCAAGGTTGTTGTTGGGAGA	106
pilT	F: GTTCCTGCTGATGTGGTGGA R: ATAACAGCGGCAGAGACTGG	109
pilA2	F: TCAAATGCTAAAGACGACGTTACAG R: TCTACTGCAAATACACCACCATCAA	104
netB	F: GGAAGGCAACTTTAAGTGGAACA R: TCAGGCCATTTCATTTTTCCGT	139
pfoA	F: CTCAGTTGCTGCTGTTCACAA R: CAAACTGTGCAACATAGGCTCC	110
plc	F: TCTTGGAGAGGCTATGCACT R: TGCGCTATCAACGGCAGTAA	79
colA	F: AGTTCCTGGAATGTGGGGAC R: TGCAAAGAACTCTGCTGTTCCT	85
16S rRNA	F: GGGGGTTTCAACACCTCC R: GCAAGGGATGTCAAGTGT	170

Expression and purification of PilA

The *pilA* gene from the strain was amplified using specific primers. These primers were designed to add BamH1 and XhoI restriction sites to the 5′ and 3′ ends of the gene, respectively. Additionally, extra codons encoding glutathione S-transferase (GST) were appended to the 3′ end of the gene. The PCR product was then ligated into the PCR cloning vector pGEX-6P-1. Subsequently, this ligated vector was introduced into competent *E. coli* BL21 cells. The *E. coli* BL21 (DE3) cells containing the PilA-pGEX-6P-1 vector were cultured and expanded in LB broth supplemented with kanamycin at a concentration of 50 μg/mL. When the OD600nm reached 0.6–0.8, the culture was transferred to an environment maintained at 16 °C. The cells were continuously shaken for a period of 15 h, during which isopropyl β-D-1-thiogalactopyranoside (Sigma-Aldrich, St. Louis, USA) was added to the culture to achieve a final concentration of 0.5 mM. The bacteria were then harvested by centrifugation and resuspended in PBS. Subsequently, the resuspended bacteria were lysed using sonication. The soluble GST-tagged proteins were finally purified using the GSTRap system (Yease, Shanghai, China).

Preparation of mouse anti-PilA polyclonal antibody

Briefly, four healthy female KM mice (6–8 weeks old) were selected for immunization. On the first day, mice were immunized via multipoint dorsal injection using a 1:1 mixture of complete Freund's adjuvant (Sigma-Aldrich, St. Louis, USA) and PilA active protein with a concentration of 1 mg/mL. On the 8th, 15th and 22nd days, the immunizations were repeated using incomplete Freund's adjuvant (Sigma-Aldrich, St. Louis, USA). After continuous injection for 4 weeks, the mouse serum was collected by aspiration. Subsequently, the aspirated serum was incubated at a temperature of 56 °C for a duration of 30 min. Finally, the serum was frozen and stored at −80 °C. All the animal experiments were conducted in accordance with the guidelines of the Animal Care and Use Committee (ACUC) of Jilin University (JLM 221407-2).

PilA expression determination

The overnight culture of *C. perfringens* ATCC13124 was subcultured at a dilution ratio of 1:100 in fresh BHI medium supplemented with a series of concentrations (0 μg/mL and 16 μg/mL) of IXN. The cultures were

allowed to grow until they reached an OD 600 nm of 1.3. DMSO was used as the solvent control. After centrifugation at 12,000 rpm for 10 min, specific volumes of the culture precipitates were suspended in SDS-PAGE loading buffer with β-mercaptoethanol (β-Me). The samples were then boiled for 10 min at 95 °C. Subsequently, the samples were separated by 12% SDS-PAGE and transferred onto a PVDF (polyvinylidene fluoride) membrane. Following blocking of the PVDF membrane with 5% nonfat dry milk, it was incubated with the pilA antibody that we had produced at a dilution ratio of 1:1000. Additionally, it was also incubated with horseradish peroxidase (HRP)-conjugated goat anti-mouse IgG (H+L) secondary antibodies at a dilution ratio of 1:1000 (Proteintech, Rosemount, IL, USA). Then, the target blots were detected using an ECL hypersensitive luminescent solution on an imager (Tanon, Shanghai, China). Finally, the densitometry of the detected blots was quantified using ImageJ software (NIH, Bethesda, USA).

Gas gangrene infection model in mice

The animal utilized were 6- to 8-week-old female BALB/c mice (Changsheng Biotechnology, Liaoning, China). Animal experiments were conducted in accordance with the guidelines of the Animal Care and Use Committee (ACUC) of Jilin University (JLM 221407-4).

For the survival rate assay, the mice were infected via intramuscular injection into the thigh muscle with a dose of 2×10^8 cfus of *C. perfringens* ATCC13124. Meanwhile, for the determination of bacteria load and histopathology, a dose of 1×10^7 cfus was used for the infection. The mice were randomly divided into two groups after infection: the WT group and IXN treatment group. Additionally, an untreated control group was also established simultaneously. In the WT + IXN group, a dose of 50 mg/kg body weight of the relevant substance was administered at intervals of 8 h for a total period of 24 h following the infection. In contrast, the WT group was given the same volume of DMSO. Subsequently, the survival rate of the mice within 60 h was calculated. In other assay, the mice were sacrificed by cervical dislocation at 24 h after the infection. The thigh muscle tissue was collected to prepare hematoxylin–eosin (HE) staining sections for histopathology observation, while the other part was homogenized for bacterial load measurement.

Statistical analysis

Statistical analyses were conducted using GraphPad Prism (version 5.0) with independent Student's *t* test. All the data are shown as the mean ± SEM for at least three replicates. The *p*-value less than 0.01 indicates that the difference is highly significant; While p-value less than 0.05 means the difference is significant; whereas a *p*-value greater than 0.05 means there was no significant difference.

Results

IXN inhibits TFP-mediated gliding motility

Previous studies have demonstrated that TFP play a crucial role in mediating the gliding motility of *C. perfringens* on BHI agar. We screened the natural compounds based on the gliding motility of *C. perfringens* ATCC13124, and found that IXN (Fig. 1A) inhibited the gliding motility of *C. perfringens* at a concentration of 8 μg/mL (Fig. 1B). Subsequently, the diameters of the gliding motility resulting from treatments with different concentrations of the

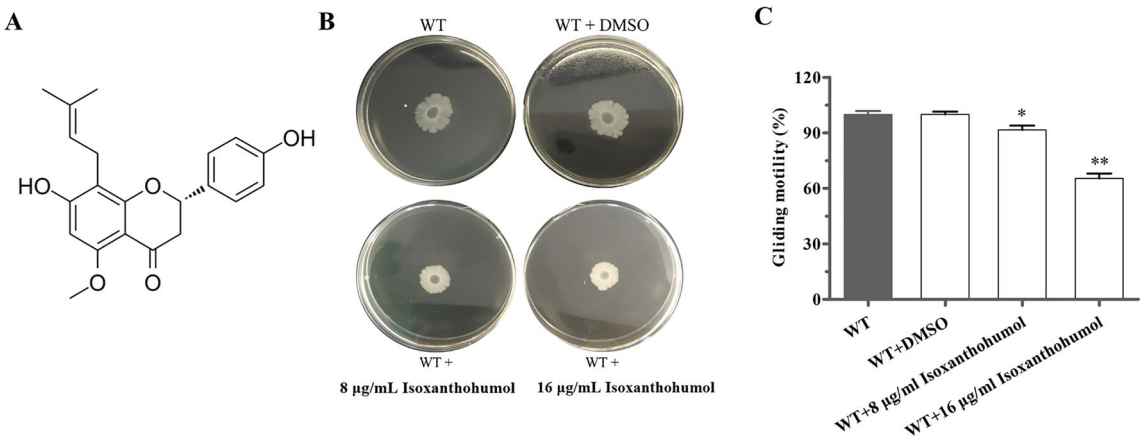

Fig. 1 IXN inhibits the gliding motility of *C. perfringens*. **A** The molecular formula of IXN. **B** The inhibitory effect of IXN on the gliding motility of *C. perfringens* was evaluated. The gliding diameter of *C. perfringens* was measured using semi-solid agar supplemented with different concentrations of IXN. **C** It was observed that the gliding motility of *C. perfringens* was significantly inhibited at a concentration of 16 μg/mL. All data are derived from at least three independent experiments. *$P < 0.05$; **$P < 0.01$

candidate compounds were measured. Which also confirmed that IXN significantly inhibited the gliding motility of *C. perfringens* (Fig. 1C).

IXN exerts no impact on the growth of C. perfringens

Both the measurement of the MIC and the growth curve were utilized to explore the effect of IXN on the growth of *C. perfringens*. As illustrated in Fig. 2A, it was evident that IXN did not have a significant effect on the growth of *C. perfringens* even when the concentration was as high as 64 μg/mL. Concurrently, the MIC results demonstrated that the MIC of IXN against *C. perfringens* 128 μg/mL (Fig. 2B). In conclusion, it can be concluded that IXN inhibits the gliding motility of *C. perfringens* via non-bactericidal or non-bacteriostatic action mechanisms.

IXN inhibits the TFP-dependent biofilm formation of C. perfringens

It has been reported that the majority bacteria exist in the form of biofilms within the natural environment, and the TFP-mediated gliding motility serves as a favorable condition for biofilm formation. Briefly, the biofilm formation of *C. perfringens* upon treatment with IXN was evaluated through crystal violet staining. As shown in Fig. 3A, the biofilm formation rate of *C. perfringens* in the control group was designated as 100%. The biofilm formation was significantly suppressed by IXN at a concentration of 8 μg/mL. Moreover, at a concentration of 16 μg/mL, the biofilm formation rate decreased by 40%. In addition, when the biofilm was diminished, the quantity of planktonic bacteria in the supernatant increased (Fig. 3B). The ratio of A_{570}/OD_{600} of the bacterial solution (Fig. 3C) illustrates the relationship between the amount of biofilm and planktonic bacteria. As shown in Fig. 3D, the number of bacteria in supernatant and within the biofilm was significantly reduced under the dual influence of H_2O_2 and IXN in comparison to the untreated group.

IXN inhibits TFP-mediated adherence of C. perfringens to Caco-2 Cells

The ability of *C. perfringens* adhesion and invasion host cells is mainly mediated by TFP [22]. Firstly, the cytotoxicity of IXN to Caco-2 cells was examined by measuring the LDH release in the co-culture system. The results indicated that IXN did not exhibit significant cytotoxicity to Caco-2 cells within the concentration of 4–64 μg/mL (Fig. 4A). As shown in Fig. 4B, the adherence rate reduced to 31% at the concentration of 16 μg/mL.

IXN down-regulates the transcription level of TFP related genes

As shown in Fig. 5A, we obtained images of the pili of *C. perfringens* ATCC13124 by using a TEM. The results demonstrated that the surface of the bacteria in the control group was rough, with a significant number of pili. The results demonstrated that the surface of the bacteria in the control group was rough, with a significant number of pili. Compared with the untreated group, IXN significantly down-regulated the expression of related genes, among which *pilC* genes had the most significant inhibitory, while *pilD* gene expression was slightly up-regulated (Fig. 5B, Fig. S1). IXN can also reduce the expression of *C. perfringens* two-component regulatory genes and its

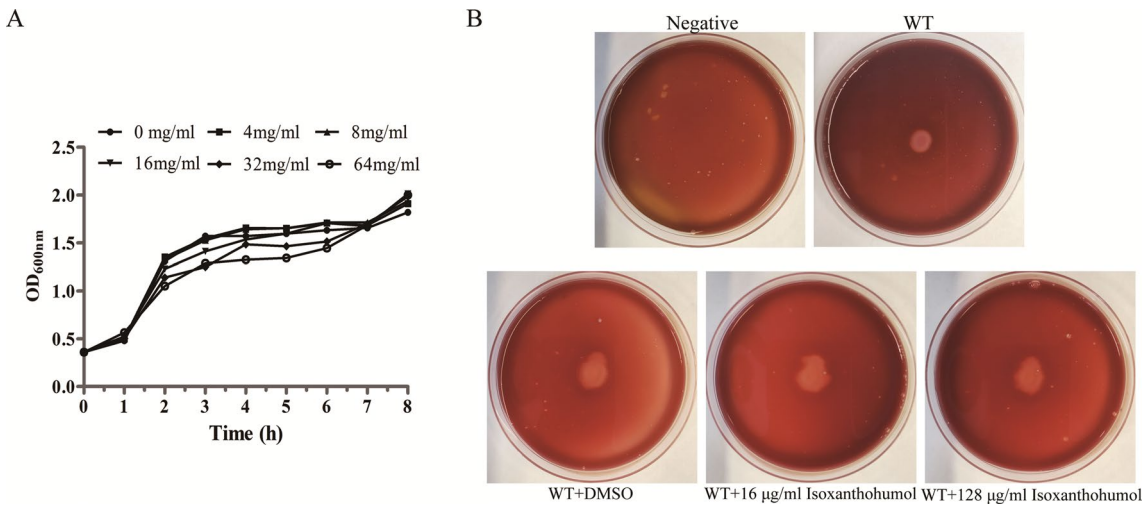

Fig. 2 IXN has no effect on the growth of *C. perfringens*. **A** The growth curve of *C. perfringens* when co-cultured with different concentrations of IXN is shown. **B** The MIC assays of *C. perfringens* against IXN were conducted. The MIC value was evaluated based on the colonies formed on the agar plates

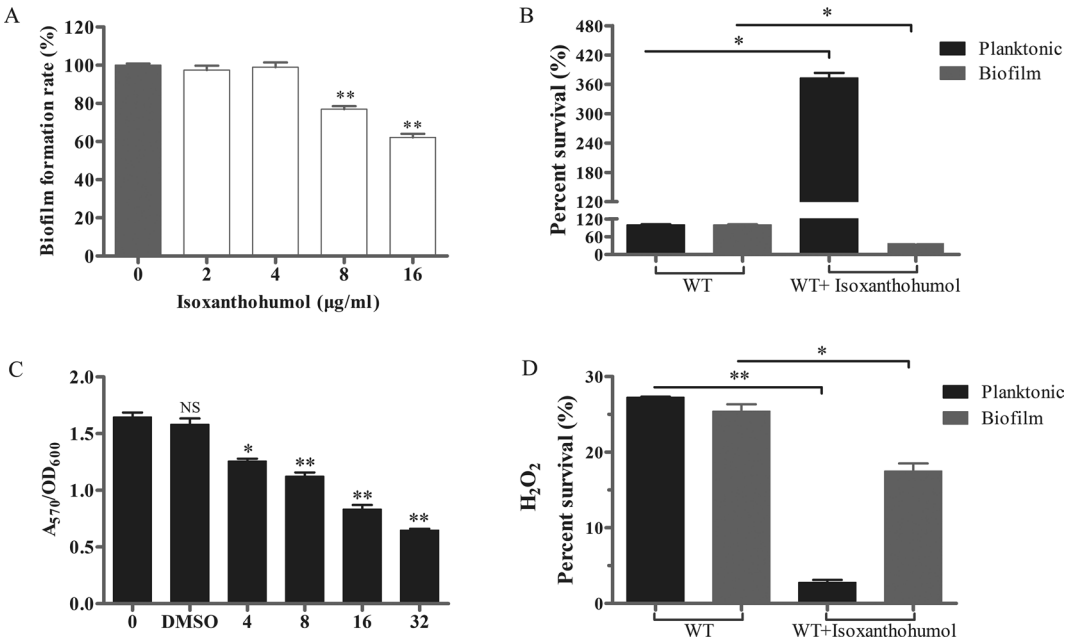

Fig. 3 IXN inhibits TFP-mediated biofilm formation of *C. perfringens*. **A** IXN inhibits the biofilm formation of *C. perfringens*. Bacterial cultures were supplemented with IXN at final concentrations of 4, 8 and 16 μg/mL and then anaerobically cultured for 120 h at 30 °C. The biofilm was measured by crystal violet staining at an absorbance of 570 nm. **B** The colony count of planktonic bacteria in the supernatant and sessile bacteria in the biofilm on BHI plates. **C** The optical density at 600 nm (OD_{600nm}) value of the planktonic bacteria in the supernatant was measured using a spectrophotometer, and the absorbance of the biofilm was measured by crystal violet staining to obtain the ratio of $A570_{nm}/OD_{600nm}$. **D** Under oxidative stimulation (simulated with H_2O_2), the number of planktonic bacteria in the supernatant or biofilm was decreased, and the sensitivity to H_2O_2 increased in the IXN group. All data are derived from at least three independent experiments. *$P < 0.05$; **$P < 0.01$; NS indicates not statistically significant

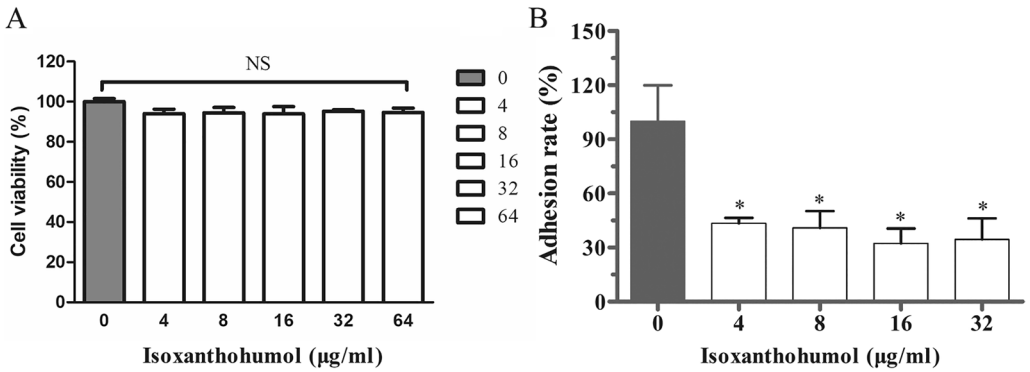

Fig. 4 **A** The cytotoxicity of IXN to Caco-2 cells was determined by LDH assay. The LDH assay was used to evaluate the cytotoxicity of IXN to Caco-2 cells. **B** IXN was shown to reduce the TFP-mediated adhesion rate of *C. perfringens* ATCC13124. All data are derived from at least three independent experiments. *$P < 0.05$; NS indicates not statistically significant

downstream genes (Fig. 5C). IXN can affect the activity of TFP by reducing the expression of PilA protein (Fig. 5D-E).

IXN protects mice infected with C. perfringens

In the survival rate experiment, gas gangrene was induced in the mice through intramuscular injection of bacteria into the left leg. In the WT + IXN group, the survival rate reached 100% within 12 h and 40% within 24 h. However, all the mice in this group eventually died within 60 h (Fig. 6A). Regarding the ocular pathological changes, the left leg muscle of the WT group exhibited different degrees of black necrosis. In contrast, the WT + IXN group only presented with significant swelling, and no

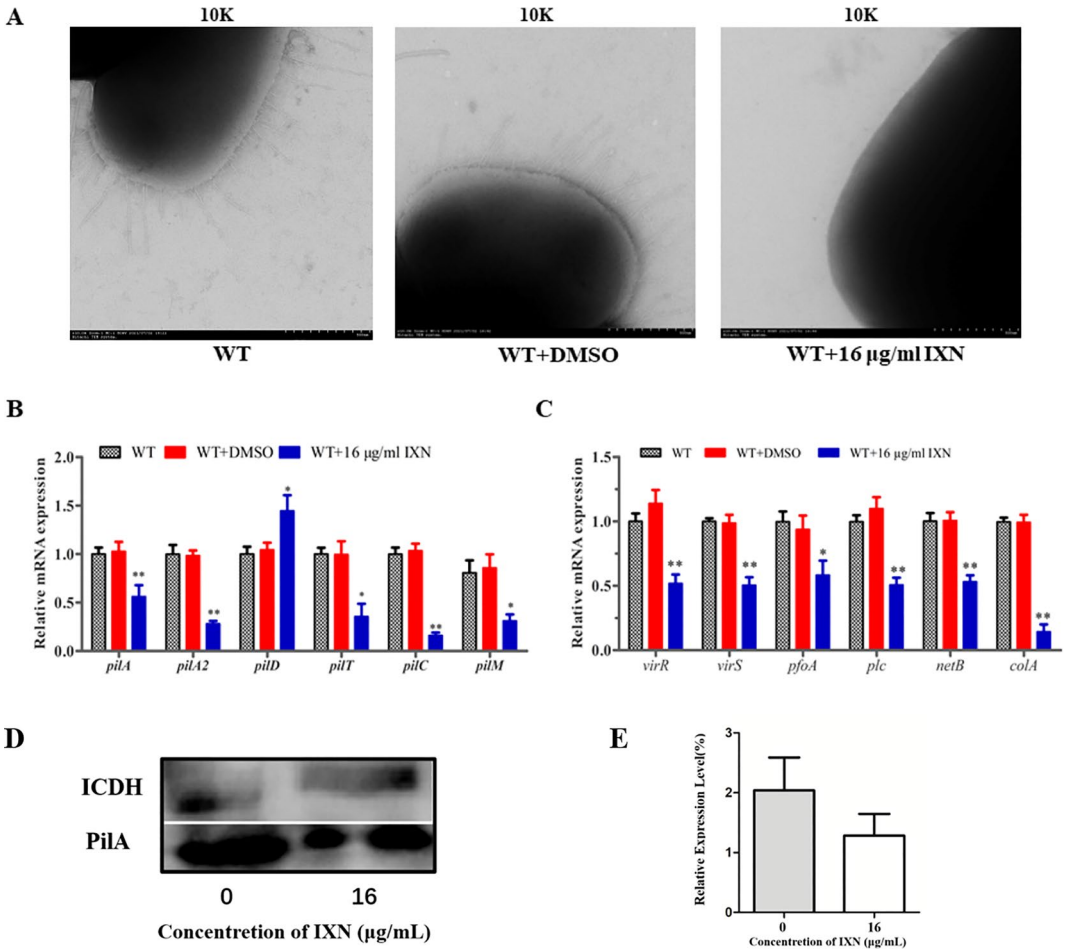

Fig. 5 IXN inhibits TFP-related genes expression and pili formation of *C. perfringens*. **A** The morphology of pili was observed under a TEM to evalute the effect of IXN on pili formation. **B** The effect of IXN on the expression of TFP-related genes was investigated. **C** The effect of IXN on the expression of two-component regulatory genes and downstream genes was also examined. All data are derived from at least three independent experiments. **P* < 0.05; ***P* < 0.01

symptoms of black necrosis were observed (Fig. 6B). In the histopathology assays, the WT group infected with *C. perfringens* displayed typical pathological damage, with a large number of leukocytes infiltrating the tissues [23]. Meanwhile, the IXN treatment group showed almost no macroscopic pathological damage to the eyes (Fig. 6C). In bacterial burden assays, the number of bacteria colonizing the tissues in the WT + IXN group was significantly lower than that in the WT group. This finding demonstrated that the survival of bacteria within the host tissue was reduced by IXN (Fig. 6D).

Discussion and conclusion

In recent decades, antibiotics have been extensively utilized in the realms of human and veterinary medicine. Nevertheless, bacteria have managed to develop resistance to nearly all the commonly available antibiotics. Even in the future, humans may face no drug available for bacterial infections [24]. Previous studies have demonstrated that certain natural compounds possess the ability to inhibit the virulence factors of bacteria, thereby lessening the occurrence of pathogen infections [25, 26]. Numerous studies have indicated that IXN exhibits favorable antiviral activity against bovine viral diarrhea mucosal disease (BVDV) and herpes simplex virus (HSV) [27]. Moreover, drug products based on IXN might have unique effects on the treatment of hepatitis. IXN has good preventive and therapeutic effects on cancer by inhibiting the function of endothelial cells [28]. Additionally, IXN also inhibits the synthesis and release of pro-inflammatory mediators in human monocyte line Mono-Mac-6, providing evidence that it may also affect tumor host crosstalk [28]. Meanwhile, studies have shown that some natural compounds can inhibit bacterial virulence factors, thereby reducing pathogen infections. Consequently, targeting bacterial virulence factors for

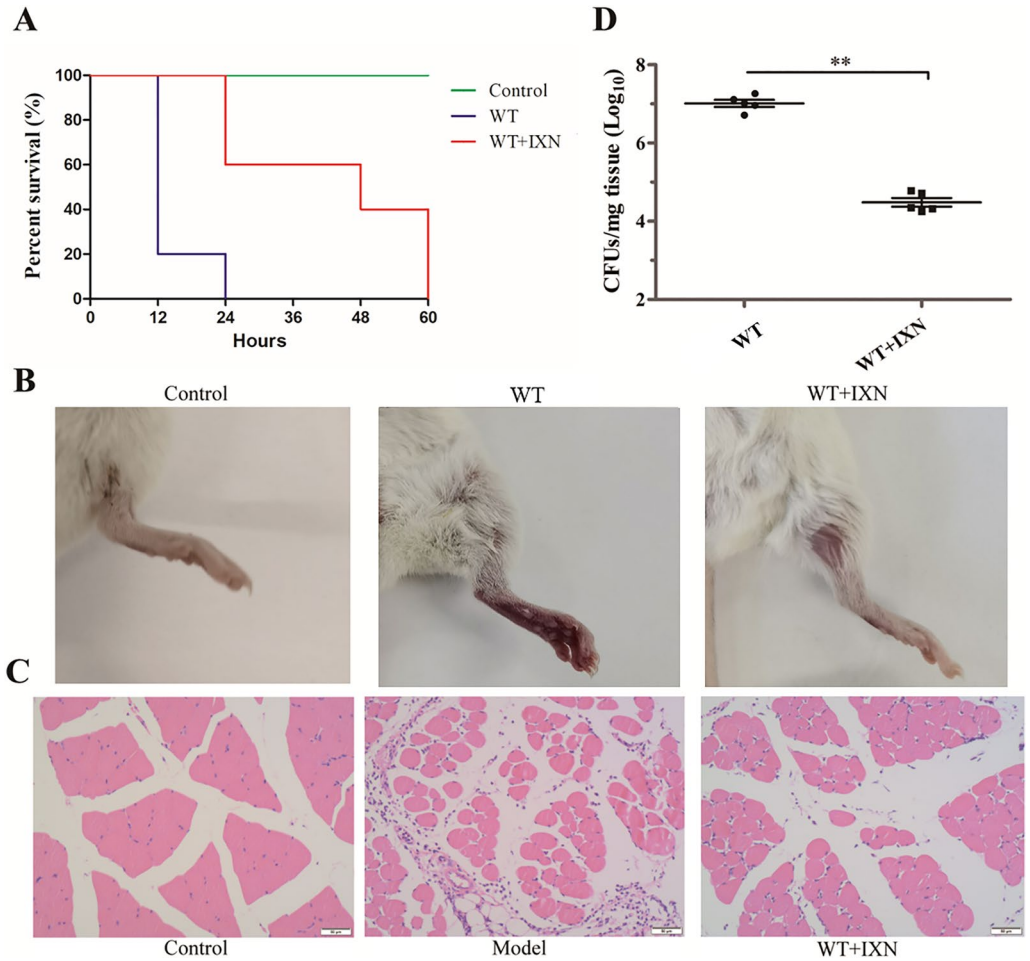

Fig. 6 IXN protective infected mice from gas gangrene. **A** IXN was found to significantly reduce the mortality of mice infected with *C. perfringens*. **B** The ocular lesions of the mice left leg muscles in each group were observed. **C** Histopathological observations of the thigh muscle tissue were conducted using hematoxylin & eosin staining (×200). **D** The bacterial load in the left leg muscles 24 h after infection was measured. *$P < 0.05$; ** $P < 0.01$

the treatment of infectious diseases presents a promising new approach in clinical treatment. Although numerous studies have demonstrated that IXN has excellent anti-inflammatory and antibacterial properties, its inhibitory effect on the TFP of *C. perfringens* as well as the underlying mechanism have not yet been reported.

We used *C. perfringens* ATCC13124 as a model strain to screen TFP inhibitors and analyzing their action mechanism. IXN, an important active ingredient derived from *Humulus lupulus Linn*, exerts a significant inhibitory effect on the transcription of TFP and related genes in *C. perfringens*. Firstly, it was demonstrated that IXN could inhibit TFP-mediated gliding motility and the function of TFP without affecting the bacteria growth. Previous studies have established that the main components of the biofilms are pili. Consequently, the inhibition of IXN on the biological functions of *C. perfringens* TFP was evaluated through biofilm formation assays and Caco-2 cell adhesion assays. The results confirmed that IXN significantly reduced bacterial adhesion and biofilm formation without cytotoxicity. In addition, TEM images revealed that IXN inhibited the morphology and synthesis of TFP on the surface of the bacteria. The transcription levels of TFP related genes (*virR*, *virS*, *pilA*, *pilD*, *pilT*, *pilC*, *pilM*) were detected by RT-PCR. The results indicated that all TFP-related encoding genes and two comment regulatory genes were significantly down-regulated except *pilD*. The low expression levels of the major *pilA* gene might lead to a reduction or even deletion of pili, thereby resulting in a decrease in biofilm formation. The reduced transcription level of *pilT* could contribute to a decline in bacterial gliding motility. Finally, the therapeutic effect of IXN on mice with gas gangrene caused by *C. perfringens* was verified through animal experiments. The results showed that IXN significantly could prolong the

survival time, improve the survival rate, alleviate the pathological damage to the thigh muscle tissue, and reduced the bacteria colonization in the muscle.

In the research, it was observed that IXN inhibits the functions mediated by TFP and exhibits favorable therapeutic effects on gas gangrene. This finding implies that the inhibition of bacterial virulence factors can serve as an effective means to combat drug-resistant bacterial infections. However, the current research still has certain limitations. IXN has poor water solubility, and continuous improvement in solubility and dosage form is needed in the future to enhance its absorption efficiency and bioavailability. The reports regarding the pharmacological activity of IXN have predominantly centered on its beneficial aspects, while the understanding of its side effects and toxicity remains insufficient. The research in this field is not yet comprehensive enough, and thus future research endeavors should place emphasis on the rational evaluation of such issues. In conclusion, IXN is a widely sourced and stable natural compound with broad application prospects in combating pathogenic bacterial infections.

Abbreviations

C. perfringens	*Clostridium perfringens*
NE	Necrotic enteritis
TFP	Type IV pili
IXN	Isoxanthohumol
TEM	Transmission electron microscopy
DMSO	Dimethyl sulfoxide
ATCC	American Type Culture Collection
ON	Overnight
OD	Optical density
MIC	Minimum inhibitory concentration
CLSI	Clinical and Laboratory Standards Institute
PBS	Phosphate-buffered saline
TSB	Tryptic soy broth
H_2O_2	Hydrogen peroxide
DMEM	Dulbecco's modified Eagle's medium
FBS	Fetal bovine serum
LDH	Lactate dehydrogenase
GST	Glutathione *S*-transferase
ACUC	Animal Care and Use Committee
β-Me	β-Mercaptoethanol
PVDF	Polyvinylidene fluoride
HRP	Horseradish peroxidase
H&E	Hematoxylin and eosin

Supplementary Information

The online version contains supplementary material available at https://doi.org/10.1186/s12934-025-02644-w.

Supplementary Material 1.

Acknowledgements
This work was supported by the National Natural Science Foundation of China (32102722, 32172806 and 31772782).

Author contributions
All authors are expected to have made substantial contributions to the conception OR design of the work; LQ and DX received project funding; SZ, DY, ZJ, WZ and LS conducted the acquisition; SZ, LS, and WZ conducted analysis, interpretation of data; DY, WZ, and LS the creation of new software used in the work; SZ, and DY have drafted the work; LQ, ZQ and DX substantively revised it. AND to have approved the submitted version (and any substantially modified version that involves the author's contribution to the study); and to have agreed both to be personally accountable for the author's own contributions and to ensure that questions related to the accuracy or integrity of any part of the work, even ones in which the author was not personally involved, are appropriately investigated, resolved, and the resolution documented in the literature.

Availability of data and materials
All data can be made available upon request to the corresponding author.

Declarations

Competing interests
The authors declare no competing interests.

Received: 31 October 2023 Accepted: 5 January 2025
Published online: 21 February 2025

References

1. Kiu R, Hall LJ. An update on the human and animal enteric pathogen *Clostridium perfringens*. Emerg Microbes Infect. 2018;7(1):141. https://doi.org/10.1038/s41426-018-0144-8.
2. Kiu R, Shaw AG, Sim K, Acuna-Gonzalez A, Price CA, Bedwell H, et al. Particular genomic and virulence traits associated with preterm infant-derived toxigenic *Clostridium perfringens* strains. Nat Microbiol. 2023;8(6):1160–75. https://doi.org/10.1038/s41564-023-01385-z.
3. Uzal FA, Navarro MA, Li J, Freedman JC, Shrestha A, McClane BA. Comparative pathogenesis of enteric clostridial infections in humans and animals. Anaerobe. 2018;53:11–20. https://doi.org/10.1016/j.anaerobe.2018.06.002.
4. Badilla-Vargas L, Pereira R, Molina-Mora JA, Alape-Girón A, Flores-Díaz M. *Clostridium perfringens* phospholipase C, an archetypal bacterial virulence factor, induces the formation of extracellular traps by human neutrophils. Front Cell Infect Microbiol. 2023;13:1278718. https://doi.org/10.3389/fcimb.2023.1278718.
5. Arseculeratne SN, Panabokke RG, Navaratnam C. Pathogenesis of necrotising enteritis with special reference to intestinal hypersensitivity reactions. Gut. 1980;21(4):265–78. https://doi.org/10.1136/gut.21.4.265.
6. Junior CAO, Silva ROS, Lobato FCF, Navarro MA, Uzal FA. Gas gangrene in mammals: a review. J Vet Diagn Invest. 2020;32(2):175–83. https://doi.org/10.1177/1040638720905830.
7. Mehdizadeh GI, Navarro M, Li J, Shrestha A, Uzal F, McClane B. Pathogenicity and virulence of *Clostridium perfringens*. Virulence. 2021;12(1):723–53. https://doi.org/10.1080/21505594.2021.1886777.
8. Soncini SR, Hartman AH, Camper GJ, Jensen RV, Melville SB. Changes in the expression of genes encoding type IV pili-associated proteins are seen when *Clostridium perfringens* is grown in liquid or on surfaces. BMC Genomics. 2020;21(1):45. https://doi.org/10.1186/s12864-020-6453-z.
9. Lepp D, Zhou Y, Ojha S, Mehdizadeh Gohari I, Carere J, Yang C, et al. *Clostridium perfringens* produces an adhesive pilus required for the pathogenesis of necrotic enteritis in poultry. J Bacteriol. 2021;203(7):e00578-e620. https://doi.org/10.1128/JB.00578-20.
10. Hendrick WA, Orr MW, Murray SR, Lee VT, Melville SB. Cyclic Di-GMP binding by an assembly ATPase (PilB2) and control of type IV pilin polymerization in the gram-positive pathogen *Clostridium perfringens*. J Bacteriol. 2017;199(10):e00034-e117. https://doi.org/10.1128/JB.00034-17.
11. Tammam S, Sampaleanu LM, Koo J, Sundaram P, Ayers M, Chong PA, et al. Characterization of the PilN, PilO and PilP type IVa pilus subcomplex. Mol Microbiol. 2011;82(6):1496–514. https://doi.org/10.1111/j.1365-2958.2011.07903.x.
12. Balasingham SV, Collins RF, Assalkhou R, Homberset H, Frye SA, Derrick JP, et al. Interactions between the lipoprotein PilP and the secretin PilQ in

Neisseria meningitidis. J Bacteriol. 2007;189(15):5716–27. https://doi.org/10.1128/JB.00060-07.
13. Varga JJ, Therit B, Melville SB. Type IV pili and the CcpA protein are needed for maximal biofilm formation by the gram-positive anaerobic pathogen *Clostridium perfringens*. Infect Immun. 2008;76(11):4944–51. https://doi.org/10.1128/IAI.00692-08.
14. Liu H, Bouillaut L, Sonenshein AL, Melville SB. Use of a mariner-based transposon mutagenesis system to isolate *Clostridium perfringens* mutants deficient in gliding motility. J Bacteriol. 2013;195(3):629–36. https://doi.org/10.1128/JB.01288-12.
15. Yang YN, Han B, Zhang MQ, Chai NN, Yu FL, Qi WH, et al. Therapeutic effects and mechanisms of isoxanthohumol on DSS-induced colitis: regulating T cell development, restoring gut microbiota, and improving metabolic disorders. Inflammopharmacology. 2024;32(3):1983–98. https://doi.org/10.1007/s10787-024-01472-5.
16. Wang F, Shin JY, Kang ES, Kim JH, Jang SI, Cho BO. Kushenol C from Sophora flavescens protects against UVB-induced skin damage in mice through suppression of inflammation and oxidative stress. Heliyon. 2023;9(12): e22804. https://doi.org/10.1016/j.heliyon.2023.e22804.
17. Watanabe Y, Fujisaka S, Morinaga Y, Watanabe S, Nawaz A, Hatta H, et al. Isoxanthohumol improves obesity and glucose metabolism via inhibiting intestinal lipid absorption with a bloom of *Akkermansia muciniphila* in mice. Mol Metab. 2023;11(77): 101797. https://doi.org/10.1016/j.molmet.2023.101797.
18. Yan YF, Wu TL, Du SS, Wu ZR, Hu YM, Zhang ZJ, et al. The antifungal mechanism of isoxanthohumol from *Humulus lupulus Linn*. Int J Mol Sci. 2021;22(19):10853. https://doi.org/10.3390/ijms221910853.
19. Waugh E. M11-A8 methods for antimicrobial susceptibility testing of anaerobic bacteria. Approved standard M11-A7 2007.CLSI
20. Broussas M, Broyer L, Goetsch L. Evaluation of antibody-dependent cell cytotoxicity using lactate dehydrogenase (LDH) measurement. Methods Mol Biol. 2013;988:305–17. https://doi.org/10.1007/978-1-62703-327-5_19.
21. Mendez M, Huang IH, Ohtani K, Ohtani K, Grau R, Shimizu T, et al. Carbon catabolite repression of type IV pilus-dependent gliding motility in the anaerobic pathogen *Clostridium perfringens*. J Bacteriol. 2008;190(1):48–60. https://doi.org/10.1128/JB.01407-07.
22. Melville S, Craig L. Type IV pili in Gram-positive bacteria. Microbiol Mol Biol Rev. 2013;77(3):323–41. https://doi.org/10.1128/MMBR.00063-12.
23. Uzal FA, Freedman JC, Shrestha A, Theoret JR, Garcia J, Awad MM, et al. Towards an understanding of the role of *Clostridium perfringens* toxins in human and animal disease. Future Microbiol. 2014;9(3):361–77. https://doi.org/10.2217/fmb.13.168.
24. Lee MH, Nuccio SP, Raffatellu M. Pathogen interference: targeting virulence factors to tackle intracellular microbes. Cell Chem Biol. 2020;27(7):765–7. https://doi.org/10.1016/j.chembiol.2020.06.017.
25. Porras G, Chassagne F, Lyles JT, Marquez L, Dettweiler M, Salam AM, et al. Ethnobotany and the role of plant natural products in antibiotic drug discovery. Chem Rev. 2021;121(6):3495–560. https://doi.org/10.1021/acs.chemrev.0c00922.
26. Yang J, Xu L, Zhou Y, Cui M, Liu D, Wang J, et al. Repurposing harmaline as a novel approach to reverse tmexCD1-toprJ1-mediated tigecycline resistance against *Klebsiella pneumoniae* infections. Microb Cell Fact. 2024;23(1):152. https://doi.org/10.1186/s12934-024-02410-4.
27. Buckwold VE, Wilson RJ, Nalca A, Beer BB, Voss TG, Turpin JA, et al. Antiviral activity of hop constituents against a series of DNA and RNA viruses. Antiviral Res. 2004;61(1):57–62. https://doi.org/10.1016/s0166-3542(03)00155-4.
28. Żołnierczyk AK, Maczka WK, Grabarczyk M, Wińska K, Woźniak E, Anioł M. Isoxanthohumol-Biologically active hop flavonoid. Fitoterapia. 2015;103:71–82. https://doi.org/10.1016/j.fitote.2015.03.007.

Publisher's Note